Coincidence of the oscillations in the dipole transition and in the persistent current of narrow quantum rings with two electrons

2008 J. Phys.: Condens. Matter 20 055214

(http://iopscience.iop.org/0953-8984/20/5/055214)

IOP Publishing Journal of Physics: Condensed Matter

J. Phys.: Condens. Matter **20** (2008) 055214 (7pp) doi:10.1088/0953-8984/20/5/055214

Coincidence of the oscillations in the dipole transition and in the persistent current of narrow quantum rings with two electrons

Y Z He and C G Bao[1]

State Key Laboratory of Optoelectronic Materials and Technologies, and Department of Physics, Sun Yat-Sen University, Guangzhou 510275, People's Republic of China

E-mail: heyanzh@mail.sysu.edu.cn and stsbcg@mail.sysu.edu.cn

Received 20 June 2007, in final form 14 December 2007
Published 17 January 2008
Online at stacks.iop.org/JPhysCM/20/055214

Abstract

The fractional Aharonov–Bohm oscillation (FABO) of one-dimensional (1D) quantum rings with two electrons has been studied. The analysis is based on the separability of the Hamiltonian into collective and internal motions. The inherent nodal structures of the internal states have been clarified; thereby these states can be classified. Some relations among them have been found. Based on the study, the evolution of the period and amplitudes of the FABO against the magnetic field B can be exactly and analytically described. Furthermore, an additional 'rule of selection' imposed on the dipole transition of the ground state has been found. Consequently, the photon energies emitted (absorbed) during the transition have only two choices. The energy difference of these two choices appears as a new kind of oscillation that matches the oscillation of the persistent current exactly. A number of analytical expressions relating the observable and dynamic parameters have been found. These equalities are helpful in the experimental determination of relevant physical quantities. The 1D model is a good approximation for the 2D rings with very narrow width. Quantitative comparison of these two models has been made.

1. Introduction

Quantum rings containing only a few electrons can now be fabricated in laboratories [1, 2]. When a magnetic field B is applied, people observed [2–4, 13] interesting physical phenomena, e.g., Aharonov–Bohm oscillation (ABO) and fractional ABO (FABO) of the ground state energy E_o and persistent current J_o. In the theoretical aspect, a number of calculations based on exact diagonalization [5–8], local-spin-density approximation [9, 10] and the diffusion Monte Carlo method [11] have been performed. These calculations can in general reproduce the experimental data. For example, in the calculation of a four-electron ring [6, 11], the period of oscillation $\Phi_0/4$ found in experiments was recovered ($\Phi_0 = hc/e$ is the flux quantum). In addition to the oscillations in E_o and J_o, the optical property has also been studied [16–20].

Due to the progress of techniques, very narrow quantum rings can be fabricated. When the electrons are confined strictly inside these rings, the two degrees of freedom normal to the circular motion surrounding the ring are very difficult to be excited. As an example, it is reminded that the excitation energy of a particle in a deep square well is very high if the width of the well is very narrow. Therefore, the two degrees of freedom can be considered as 'frozen'. And the very narrow rings can be considered as one-dimensional (1D). Whether a two-dimensional ring with a harmonic-like confinement $\propto \alpha(r - r_o)^2$ is close to a 1D ring has been studied in [21], where α measures how thin the ring would be. When $\alpha \geqslant 20$, it was found that the low-lying spectra of the two model are close to each other as shown in figures 3(a) and (b) of [21]. A similar evaluation on the wavefunctions has been made in [24], where the low-lying states are found not to contain radial excitation. And [24] also shows that their radial distribution is very thin if α is large as expected. These evaluations reveal that the 1D ring is a good approximation for very narrow rings, the thinner the ring, the better the approximation. Thus the study of the 1D model is meaningful.

Although there are many literatures dedicated to the study of 1D rings, a study in an analytical way is scarce. An important feature of 1D rings is the separability of

[1] Author to whom any correspondence should be addressed.

the Hamiltonian. This feature would facilitate greatly the theoretical analysis because the internal motion can be thereby separated. The characters of the internal states have also been scarcely studied. The scope of this paper is limited to the narrow rings containing two electrons (2-e) and threaded by a magnetic field (perpendicular to the plane of the ring) under the 1D model. The first aim is to find out the character of the internal states, to classify them and to make clear the relations among them. Based on the internal states, the period of the FABO and its variation can be described analytically as shown below. The second aim is to study the relation between the dipole transitions and the persistent current. This is a topic that has not yet been studied before. For 2-e narrow rings, it was found in this paper that the photons emitted (absorbed) by the ground state during the dipole transition have only two choices of energy (accordingly the dipole radiation has only two frequencies). Furthermore, it was found that the energy difference of the two choices is exactly equal to hJ_o where h is the Planck's constant. In other words the energy difference appears as an oscillation which matches exactly the oscillation of J_o in accord with the variation of the strength of the magnetic field. Numerical calculation and analytical analysis are reported as follows.

2. Hamiltonian

We consider a 1D ring with radius R containing two electrons lying on the X–Y plane, the Hamiltonian reads

$$H = T + V_{12} + H_{\text{Zeeman}}$$
$$T = \sum_{j=1}^{N} G\left(-\mathrm{i}\frac{\partial}{\partial\theta_j} + \Phi\right)^2, \qquad G = \frac{\hbar^2}{2m^*R^2} \tag{1}$$

where m^* is the effective mass, θ_j is the azimuthal angle of the jth electron, Φ is equal to $\pi R^2 B/\Phi_0$, B is a magnetic field goes through and perpendicular to the X–Y plane, V_{12} is the e–e Coulomb interaction, $H_{\text{Zeeman}} = -S_Z\mu\Phi$ is the well-known Zeeman energy, S_Z is the Z-component of the total spin S, μ is equal to $\frac{g^*\mu_B}{\pi R^2\Phi_0}$ and is the Bohr magneton and g^* is the effective g-factor. The interaction is adjusted as $V_{12} = e^2/(2\varepsilon\sqrt{d^2 + R^2\sin^2((\theta_1-\theta_2)/2)})$, where ε is the dielectric constant and the parameter d is introduced to account for the effect of finite width of the ring [7].

A set of basis functions $\phi_{k_1k_2} = \mathrm{e}^{\mathrm{i}(k_1\theta_1+k_2\theta_2)}/2\pi$ is introduced to diagonalize the Hamiltonian. The k_1 and k_2 must be integers to assure the periodicity and the total orbital angular momentum $L = k_1 + k_2$ is conserved. $\phi_{k_1k_2}$ must be further (anti-)symmetrized when $S = 0(1)$. More than two thousand basis functions are adopted so that relevant solutions are sufficiently accurate (having at least six effective digits).

3. Separability and related consequence

3.1. Separability of the eigenenergies and eigenstates

Let $\theta_C = (\theta_2+\theta_1)/2$, and $\varphi = \theta_2 - \theta_1$. Then the Hamiltonian can be separated as

$$H = H_{\text{coll}} + H_{\text{int}} \tag{2}$$

where

$$H_{\text{coll}} = \frac{1}{2}G\left(-\mathrm{i}\frac{\partial}{\partial\theta_C} + 2\Phi\right)^2 + H_{\text{Zeeman}} \qquad \text{and}$$
$$H_{\text{int}} = 2G\left(-\mathrm{i}\frac{\partial}{\partial\varphi}\right)^2 + V_{12}.$$

They are for the collective and internal motions, respectively.

The separability is a well-known feature [5, 14, 15]. Due to the separability, each eigenenergy E can be exactly divided as a sum of three terms

$$E = \tfrac{1}{2}G(L+2\Phi)^2 + E_{\text{int}} - S_Z\mu\Phi \tag{3}$$

where the first term is the kinetic energy of collective motion, E_{int} is the internal energy and the last term is the Zeeman energy.

On the other hand, since the basis function is separable and can be rewritten as

$$\phi_{k_1k_2} = \frac{1}{2\pi}\mathrm{e}^{\mathrm{i}L\theta_C}\mathrm{e}^{\mathrm{i}\frac{1}{2}(k_2-k_1)\varphi} \tag{4}$$

the spatial part of each eigenstate Ψ with the good quantum number L is strictly separable as $\Psi = \frac{1}{\sqrt{2\pi}}\mathrm{e}^{\mathrm{i}L\theta_C}\psi_{\text{int}}$. The first part of Ψ describes the collective motion, while the second part ψ_{int} is a superposition of $\mathrm{e}^{\mathrm{i}\frac{1}{2}(k_2-k_1)\varphi}$ and is a normalized internal state depending only on φ. In particular, neither E_{int} nor ψ_{int} depends on B (or Φ).

3.2. Classification of ψ_{int}

The period of the internal states as shown in equation (4) depends on $(k_2-k_1)\varphi/2$. When L is even (odd), $(k_2-k_1)/2$ is an integer (half-integer) and the period of φ is 2π (4π). Therefore, the periodicity of ψ_{int} have two choices depending on $(-1)^L$. Together with the two choices in S, there are totally four types of internal states. These types can be labelled by $((-1)^L, S) = (1,0), (-1,0), (-1,1)$ and $(1,1)$, or simply by a, b, c and d, respectively. The internal states of type a are denoted as ψ_a, ψ_{a^*}, ... and the associated internal energies as $E_a < E_{a^*}$, ... and so on. The features of these four types are given below.

3.3. Persistent current

A noticeable outcome of the separability is that the persistent current J can be written in an analytical form. Let J_1 be the current of particle e_1. The current is defined based on the conservation of matter and it reads as in [5]

$$J_1 = \frac{1}{2}g\int \mathrm{d}\theta_2\left[\Psi^*\left(-\mathrm{i}\frac{\partial}{\partial\theta_1} + \Phi\right)\Psi + \text{c.c.}\right] \tag{5}$$

where $g = \hbar/(m^*R^2)$.

Since J_1 does not depend on the azimuthal angle θ_1, J_1 is equal to $\frac{1}{2\pi}\int J_1\,\mathrm{d}\theta_1$. Thus the total current $J = J_1 + J_2$ is

$$J = \frac{1}{4\pi}g\int \mathrm{d}\theta_1\mathrm{d}\theta_2\left[\Psi^*\left(-\mathrm{i}\frac{\partial}{\partial\theta_1} - \mathrm{i}\frac{\partial}{\partial\theta_2} + 2\Phi\right)\Psi + \text{c.c.}\right]. \tag{6}$$

When the arguments are changed to θ_C and φ, due to $\frac{\partial}{\partial\theta_1} + \frac{\partial}{\partial\theta_2} = \frac{\partial}{\partial\theta_C}$ and the separability of Ψ, the integration over θ_C and φ can be performed analytically. Thus we have

$$J = g(L + 2\Phi)/2\pi. \tag{7}$$

This expression of J, together with equation (3), tells us transparently that the (F)ABO of the ground state energy E_o and the persistent current J_o match with each other exactly. They contain the same factor $(L + 2\Phi)$. Therefore they are governed by the same mechanism, namely, the transition of L_o in accord with the variation of Φ. In particular, E_o and J_o are related to each other directly as

$$E_o = m^*(\pi R J_o)^2 + E_{int} - S_Z\mu\Phi.$$

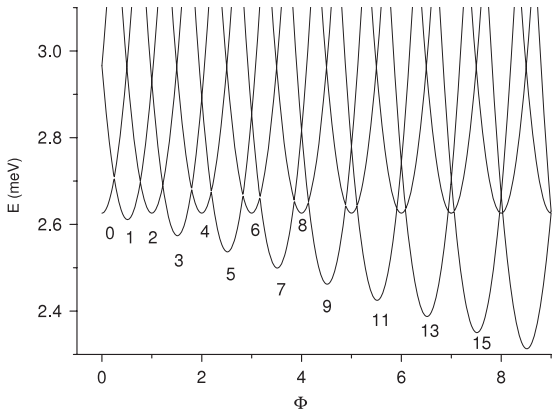

Figure 1. Low-lying levels of a 2-e ring against Φ in the FABO region. The numbers by the curves are $-L_o$. $R = 30$ nm is assumed.

3.4. Dipole transition

A lower state may jump to a higher state by absorbing a photon via the dipole transition, or vice versa. Let the initial and final states be denoted as $\Psi_{(i)}$ and $\Psi_{(f)}$, respectively, with angular momenta $L_{(i)}$ and $L_{(f)}$. For dipole transitions, only $L_{(f)} = L_{(i)} \pm 1$ is allowed. The photon energy $\hbar\omega$ of the dipole transition is equal to the energy difference of the states. The probability of dipole transition reads [22]

$$P^{(f)}_{(i),\pm} = \frac{2e^2}{3\hbar}(\omega_\pm/c)^3 R^2 |A^{(f)}_{(i),\pm}|^2 \tag{8}$$

where the additional subscript $\pm$ is used to distinguish the two cases $L_{(f)} = L_{(i)} \pm 1$, (f) and (i) denote the final and initial states, respectively,

$$A^{(f)\pm}_{(i)} = \langle\Psi_{(f)\pm}|e^{\pm i\theta_1} + e^{\pm i\theta_2}|\Psi_{(i)}\rangle. \tag{9}$$

Since $e^{\pm i\theta_1} + e^{\pm i\theta_2} = 2e^{\pm i\theta_C}\cos(\varphi/2)$ and the eigenstates are separable, the above equation can be rewritten as

$$A^{(f)\pm}_{(i)} = \delta_{L_{(f)},L_{(i)}\pm1} 2\langle\psi^{(f)\pm}_{int}|\cos(\varphi/2)|\psi^{(i)}_{int}\rangle. \tag{10}$$

This equation implies that not only the collective motion would gain (lose) a unit of angular momentum but also the internal state would undergo a change caused by the operator $2\cos(\varphi/2)$ during the dipole transition. This formula together with the knowledge on the internal states would facilitate the following analysis.

4. Numerical results and analysis

Numerical calculation has been performed with the parameters $m^* = 0.063m_e$, $\varepsilon = 12.4$ (for InGaAs) and $d = 0.02R$. The units meV, nm, T and Φ_0 are used. Accordingly, $G = 604.8/R^2$ and $\mu = 33.53/R^2$. Related eigenenergies and eigenstates are obtained after the diagonalization.

The low-lying spectrum is plotted in figure 1. Since the ground state energy would have the factor $|L+2\Phi|$ minimized (refer to equation (3)), its angular momentum L_o would jump step by step in accord with the variation of Φ. This is clearly shown in the figure. And the (F)ABO of the ground state energy E_o is thereby induced.

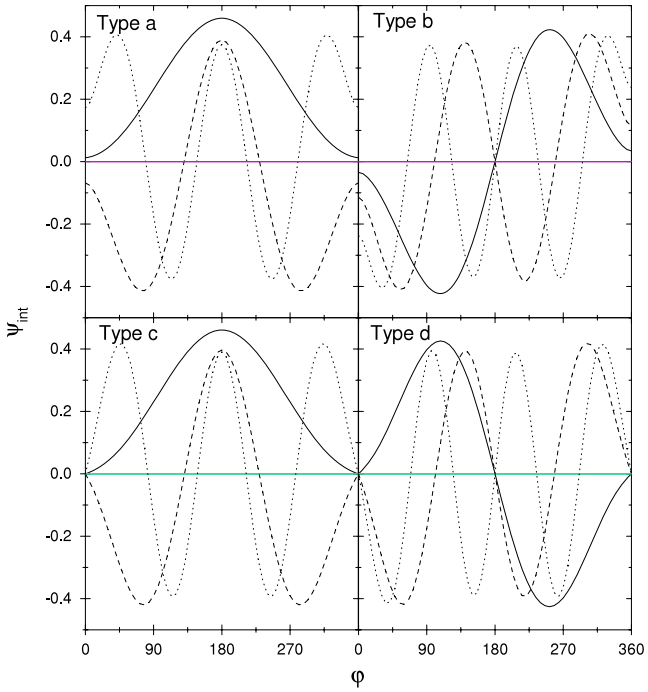

Figure 2. Four types of ψ_{int} against φ, $R = 30$ nm. The lowest three of each type is shown. The higher state has more nodes.
(This figure is in colour only in the electronic version)

The internal energies can be directly extracted from the eigenenergies. When only low-lying levels are taken into account (excitation energy <10 meV), only eight internal states are involved (they generate the whole low-lying spectra). They are classified into four types and they are just the lowest two of each type. For example, when $R = 30$, their energies are listed in table 1 and their wavefunctions are plotted in figure 2.

Due to the e–e repulsion, a dumb-bell shape (i.e., $\varphi = \pi$) is advantageous in energy. However, a rotation of this geometry by π is equivalent to an interchange of particles. The rotation will create $(-1)^L$ and the interchange will create $(-1)^S$ from the wavefunction. Therefore, the equivalence leads

Table 1. The lowest and second lowest internal energies (in meV) of type a–d, $R = 30$ nm.

Type	a	b	c	d
$E_{\rm int}$	2.632	4.268	2.634	4.282
$E^*_{\rm int}$	6.406	9.066	6.455	9.194

to a constraint. Accordingly the dumb-bell shape is accessible only to the states with $L + S$ even (i.e., only to type a and c). Otherwise, the states would have an inherent node at the dumb-bell shape and therefore be higher in energy as shown in table 1, where $E_a \ll E_b$, $E_c \ll E_d$ and $E_a \approx E_c$. In figure 2 the patterns of type a and c are one-to-one similar and they all have a peak at $\varphi = \pi$ implying the existence of the dumb-bell shape. The patterns of type b and d are one-to-one similar and they all have an inherent node at $\varphi = \pi$ implying the prohibition of the dumb-bell shape. It is noticeable that type b and c are not continuous at $\varphi = 0$ and 2π due to their special periodicity. It was found that the internal states of all the ground states are either ψ_a or ψ_c without exceptions due to their dumb-bell shape accessibility. On the other hand, the excited internal states will contain more additional nodes implying a more vigorous internal motion as shown in the figure. When the dynamic parameters vary in reasonable ranges, the qualitative features of figure 2 remain the same.

It is noted that $E_c \approx E_a$ and they are both much lower than E_b and E_d. If the Zeeman energy is negligible (Φ is small), both ψ_c and ψ_a would have similar chances to appear in the ground states. Accordingly, $L_{\rm o}$ of the ground state can be either odd or even. In this case, the increase of Φ will lead to a decrease of $L_{\rm o}$ step by step, each step by one. This leads to an oscillation with the period $\Phi = 1/2$ (due to the factor $L + 2\Phi$ in equation (3)). Accompanying the even–odd transition of $L_{\rm o}$, the total spin of the ground state $S_{\rm o}$ undergoes a singlet–triplet transition. However when Φ is larger than a critical value $\Phi_{\rm crit}$, only $S_{\rm o} = 1$ states can be the lowest due to the strong Zeeman effect. Accordingly, $L_{\rm o}$ must be odd. In this case, when Φ varies, $L_{\rm o}$ jumps each step by two and the period of oscillation becomes $\Phi = 1$. The region $\Phi < (>)\Phi_{\rm crit}$ is called the FABO (ABO) region, where the period is a fraction (an integer).

Examples of the ground state persistent current $J_{\rm o}$ are shown in figure 3, where the period of oscillation is exactly the same as that of $E_{\rm o}$.

From the above derivation, we know that the function $\cos(\varphi/2)$ is crucial to the dipole transition. By analysing the numerical data, we found numerically that

$$\begin{aligned} \tilde{N}(\cos(\varphi/2)\psi_a) &= \psi_b + \xi_a, \\ \tilde{N}(\cos(\varphi/2)\psi_c) &= \psi_d + \xi_c \end{aligned} \tag{11}$$

where $\tilde{N}$ is the operator of normalization, both ξ_a and ξ_c are very small functions and depend on the dynamic parameters very weakly. For example, when R varies from 30 to 90, the weights of ξ_a and ξ_c vary from 0.0004 to 0.0002. They are so small that they in fact can be neglected. Since $\cos(\varphi/2)$ contains a node at the dumb-bell shape, it may cause a change of type. If the initial state belongs to type a (c), the final state must belong to b (d). Since $\cos(\varphi/2)$ contains only one node inside the domain $[0, 2\pi]$, it can not cause a serious excitation. Naturally, if the initial state is ψ_a (ψ_c), the final state should be essentially ψ_b (ψ_d) because the latter has just one node more. This explains the above approximate equalities. They provide an additional 'rule of selection' for the dipole transition of the ground state; namely, the transition of the internal state has only one specified choice. Together with the two choices $L_{\rm (f)} = L_{\rm (i)} \pm 1$ in collective rotation, the dipole transition of the ground state concentrates only on two final states. Accordingly, the related photon has only two choices of energy

$$\begin{aligned} \hbar\omega_\pm &= E_{\rm (f)\pm} - E_{\rm (i)} \\ &= G\tfrac{1}{2}(1 \pm 2(L_{\rm o} + 2\Phi)) + \Delta_\alpha \end{aligned} \tag{12}$$

where $\alpha = a$ or c depends on the initial state. $\Delta_a = E_b - E_a$ and $\Delta_c = E_d - E_c$ and they are the differences of internal energies. Evidently, since $\hbar\omega_\pm$ contains the factor $L_{\rm o}+2\Phi$, the oscillation of $\hbar\omega_\pm$ matches the oscillation of $E_{\rm o}$ and $J_{\rm o}$ exactly as shown in figure 3. It turns out that Δ_α/G depends on R very weakly and thus $\hbar\omega_\pm$ is nearly proportional to R^{-2}. It implies that a very small ring will have a very large probability of transition.

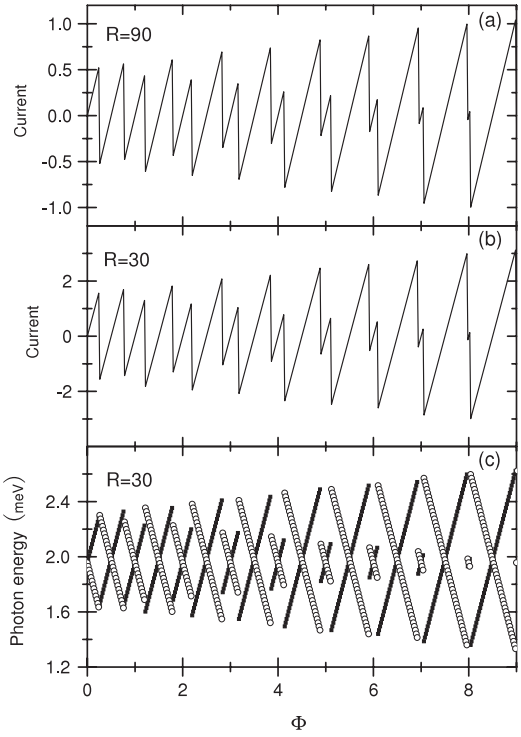

Figure 3. The oscillation of the persistent current and the two photon energies of the ground states against Φ. The unit of current is $10^{-5}C/R$, where C is the velocity of light. In the lowest panel, the black square (white circle) denotes $\hbar\omega_+$ ($\hbar\omega_-$), namely, the energy associated with $L_{\rm o}$ to $L_{\rm o} + 1$ ($L_{\rm o} - 1$) transition.

5. Analytical description of the Aharonov–Bohm oscillation

The oscillation in the FABO region is complicated as shown in figures 1 and 3, where a longer period is followed by a shorter

period and these periods vary with Φ. However, since we have the analytical expression of E_o, the variation of the period can be studied in an analytical way. In figure 1 the abscissa Φ can be divided into segments each with a specific L_o. Inside each segment E_o is given by a piece of a parabolic curve. At the border of two neighbouring segments the two related E_o are equal. From the equality and based on equation (3), the right and left boundaries of a segment can be obtained as

$$\Phi_{\text{right}}(L_o) = (1-(\mu/2G)^2)^{-1}[1-\mu(E_c-E_a)/G^2-2L_o + (-1)^{L_o}(2(E_c-E_a)+\mu(L_o-1/2))/G]/4 \quad (13)$$

$$\Phi_{\text{left}}(L_o) = (1-(\mu/2G)^2)^{-1}[-1-\mu(E_c-E_a)/G^2-2L_o - (-1)^{L_o}(2(E_c-E_a)+\mu(L_o+1/2))/G]/4 \quad (14)$$

where the flux Φ is assumed to be positive and $L_o \leqslant 0$ and $\Phi_{\text{right}}(L_o) = \Phi_{\text{left}}(L_o-1)$. When Φ is given, the associated L_o can be found from the inequality $\Phi_{\text{left}}(L_o) \leqslant \Phi \leqslant \Phi_{\text{right}}(L_o)$. Once the relation between L_o and Φ is clear, every details of the FABO can be analytically and exactly explained via equations (3), (7) and (12).

The length of a segment is just the period of Φ and it reads

$$d_{L_o} = \Phi_{\text{right}}(L_o) - \Phi_{\text{left}}(L_o) = (1-(\mu/2G)^2)^{-1}[1+(-1)^{L_o}(2(E_c-E_a)+\mu L_o)/G]/2. \quad (15)$$

Equation (15) gives a precise description of the varying period in the FABO region. In this formula, $E_c - E_a$ is very small (refer to table 1), $\Phi \geqslant 0$ and $L_o \leqslant 0$. Therefore, when Φ increases, the factor $(2(E_c-E_a)+\mu L_o)$ becomes more negative and accordingly d_{L_o} becomes shorter (longer) if L_o is even (odd). Furthermore, the extremum in each segment can be found. For example, the maximal current in a segment is $g(L_o+2\Phi_{\text{right}})/2\pi$ and the minimum of the ground state energy in a segment is $E_{\min} = E_c - \mu^2/8G + \mu L_o/2$ (if $S_o = 1$) or just $E_{\min} = E_a$ (if $S_0 = 0$).

When Φ is small, $|L_o|$ should be small. In this case, equation (15) leads to $d_{L_o} \approx 1/2$ as mentioned above.

When Φ becomes sufficiently large, L_o will become very negative and the segments with L_o even will disappear due to their lengths $d_{L_o} \leqslant 0$. We can define a critical odd integer L_{crit} so that $d_{L_{\text{crit}}-1} \leqslant 0$ while $d_{L_{\text{crit}}+1} > 0$, thereby the critical flux separating the FABO and ABO region can be defined as

$$\Phi_{\text{crit}} = \Phi_{\text{left}}(L_{\text{crit}}). \quad (16)$$

Once $\Phi > \Phi_{\text{crit}}$, L_o remains odd and the system keeps polarized ($S = 1$). Let I_X be the largest even integer smaller than $-(G+2(E_c-E_a))/\mu$. From equation (15), it turns out that $L_{\text{crit}} = I_X + 1$. With our parameters, we have $L_{\text{crit}} = -19$ and accordingly $\Phi_{\text{crit}} = 9.003$ (refer to figure 1). Both L_{crit} and Φ_{crit} depend on R very weakly but sensitively on the effective mass m^*.

In the ABO region ($\Phi > \Phi_{\text{crit}}$), equations (14) and (15) do not hold. Instead we have $\Phi_{\text{right}} = -(L_o-1)/2$, $\Phi_{\text{left}} = -(L_o+1)/2$ and $d_{L_o} = 1$. Thus the normal ABO recovers. Evaluated from equation (7), the magnitude of current is from $-g/2\pi$ to $g/2\pi$ (for a comparison, it is from $-g/4\pi$ to $g/4\pi$ for 1-e rings). From equation (12) the photon energies $\hbar\omega_+$ is from $\Delta_c - G/2$ to $\Delta_c + 3G/2$. At the same time $\hbar\omega_-$ is from $\Delta_c + 3G/2$ to $\Delta_c - G/2$.

6. Relations between the photon energies and other physical quantities

Since the emitted (absorbed) dipole photon of the ground state has only two frequencies as given in equation (12), we define $\Delta_{\hbar\omega} = \hbar(\omega_+ - \omega_-)$. Due to equation (12) and (7),

$$\Delta_{\hbar\omega} = hJ_o \quad (17)$$

where h is the Planck's constant and J_o is the persistent current of the ground state. Since J_o is oscillating against Φ, this equation shows that $\Delta_{\hbar\omega}$ is also oscillating against Φ. And these two oscillations match with each other exactly. Since photon energies can be more accurately measured, equation (17) provides a way to measure the current in high precision. Incidentally, the above formula is a generalization of the formula $\Delta_{\hbar\omega} = 2hJ_o$ for 1-e rings.

The maxima of $\Delta_{\hbar\omega}$ measured in the ABO and FABO regions, respectively, read

$$(\Delta_{\hbar\omega})^{\text{AB}}_{\max} = 2G \quad (18)$$

$$(\Delta_{\hbar\omega})^{\text{FAB}}_{\max} = 2G(L_o + 2\Phi_{\text{right}}). \quad (19)$$

Obviously, equation (18) provides a way to determine G and m^* can be thereby obtained. Equation (19) can be rewritten as

$$E_c - E_a = (G-\mu L_o)/2 - (2G-\mu)/(4G)(\Delta_{\hbar\omega})^{\text{FAB}}_{\max} \quad (20)$$

it can be used to determine $E_c - E_a$. Furthermore, we define

$$\Gamma_{\hbar\omega} = \hbar(\omega_+ + \omega_-) = G + 2\Delta_\alpha. \quad (21)$$

Once G has been found, equation (21) can be used to determine Δ_a and Δ_c. Once the internal energies have also been found, the spectrum can be found via equation (3).

7. Quantitative comparison of the 1D and 2D models

The above discussion is based on the 1D model. Since the radial excitation in very thin rings is frozen as shown in [24], therefore the 1D model would be a good approximation. Nonetheless, it would be more convincing if a quantitative estimation is made. For this purpose, a 2D model with a square well $U(r)$ is introduced, where $U(r) = 0$ if $r_A \leqslant r \leqslant r_B$, or $U(r) = +\infty$ otherwise. In addition to the above basis functions $e^{ik\theta}$ for the azimuthal motion, a set of radial basis functions $f_n(\zeta)$ is introduced. Where n is an integer $\geqslant 1$, $\zeta = \pi[r-(r_B+r_A)/2]/(r_B-r_A)$, and $f_n(\zeta) = \cos(n\zeta)$ if n is odd, or $\sin(n\zeta)$ if n is even. They are defined only inside the domain from r_A to r_B, and they are zero at the border as required. In other words, the electrons are strictly confined in the annular region. Then, the Hamiltonian is diagonalized with these basis functions. The convergency of the calculated eigenenergies is fine, four effective figures can be obtained even the total number of basis functions is not larger than one thousand. The eigenenergies of two types of states with different r_A and r_B are listed in tables 2 and 3. For each case the excitation energies of the three lowest excited states

Table 2. The excitation energies $E_i - E_1$ (in meV) of the low-lying $S = 0$ and $L = 0$ states of a 2D ring with inner and outer radii r_A and r_B (in nm). Those from the 1D model with $R = (r_B + r_A)/2$ are listed in the fourth and seventh columns for a comparison. $B = 0$ is assumed.

(r_A, r_B)	(15, 45)	(27, 33)	1D($R = 30$)	(70, 100)	(83, 87)	1D($R = 85$)
$E_2 - E_1$	3.811	3.791	3.774	0.658	0.654	0.654
$E_3 - E_1$	9.268	9.696	9.626	1.568	1.562	1.559
$E_4 - E_1$	16.294	17.796	17.605	2.750	2.747	2.739

Table 3. The same as table 2 but for the $S = 1$ and $L = 1$ states. $B = \Phi_0/(2\pi R^2)$ is assumed.

(r_A, r_B)	(15, 45)	(27, 33)	1D($R = 30$)	(70, 100)	(83, 87)	1D($R = 85$)
$E_2 - E_1$	3.977	3.831	3.821	0.658	0.654	0.654
$E_3 - E_1$	10.152	9.922	9.894	1.570	1.562	1.561
$E_4 - E_1$	18.499	18.479	18.425	2.759	2.748	2.745

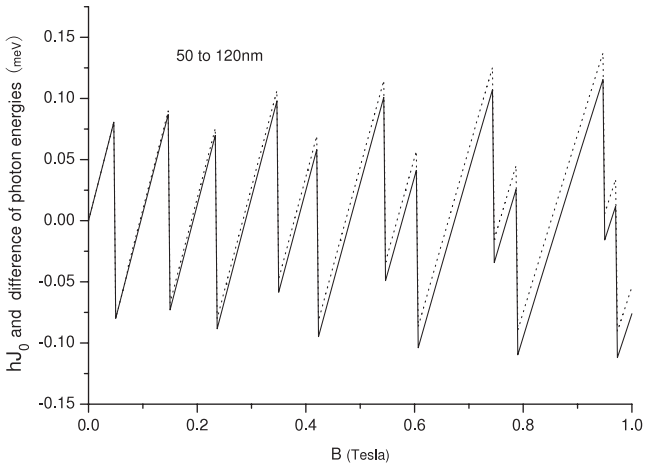

Figure 4. Evolution of hJ_o (solid line) and $\Delta_{\hbar\omega}$ (dotted line) against B for a 2-e ring with $r_a = 50$ and $r_b = 120$ nm.

are given. The absolute energies are not comparable due to having different energies in radial motion (although not yet excited). However, the excitation energies associated with the same average radius $(r_B + r_A)/2$ but with different widths $r_B - r_A$ are comparable because they are essentially contributed by the excitation of azimuthal motion. They can compare directly with those from the above 1D model.

As shown by columns 5–7 of the two tables, in accord with the decrease of the width, the 2D results tend to the corresponding 1D results. Even when the ring is small (columns 2–4), the tendency is still clear.

In addition to the energies, let us evaluate how the other features of the 1D model are affected by the width. A noticeable relation arising from the 1D model is the formula $\Delta_{\hbar\omega} = hJ_o$. Now we use the above 2D model to calculate both sides of the formula numerically, where J_o is now the total angular current. When the width of the ring is broad, $\Delta_{\hbar\omega}$ and hJ_o both as functions of B are slightly different from each other as shown in figure 4. However, when the width becomes smaller, say $r_b - r_a < 30$, the two curves overlap. Thus equation (17) works very well for two-dimensional narrow rings. Therefore, the 1D model is a good approximation for very narrow rings.

8. Conclusions

In summary, the 1D ring containing two electrons has been studied. This model is a good approximation for very narrow rings.

(i) We have classified the internal states into four types according to S and $(-1)^L$ and their features have been studied. The wavefunctions of each type have their specific inherent nodal structure and periodicity. The inherent nodal structure is imposed by symmetry and is associated with the prohibition of the dumb-bell shape. In general, for few-body systems, the inherent nodal structure is a fundamental character of a quantum state. These structures provide an objective base for the classification of states. And the spectra are thereby decisively affected [12, 23].

(ii) A number of formulae relating the physical quantities have been established (e.g., the one relating E_o and J_o). Some relations between the internal states have also been found. The finding equation (11) behaves as an additional 'rule of selection' imposing on the dipole transition of the ground state. Consequently, the transition concentrates only on two final states.

(iii) The finding equation (17) relates the dipole transition to the persistent current J_o. It implies that the oscillation of $\Delta_{\hbar\omega}$ matches J_o exactly. Thus equation (17) provides a way of precise measurement of the current. Furthermore, a number of formulae relating the dynamic parameters and observables have been established.

(iv) The period of the FABO is difficult to be described because it varies with B. Nonetheless, we have succeeded to derive an analytical equation (15) to describe the period exactly.

The discussion in this paper is making use of the separability of the Hamiltonian and is based on the inherent nodal structures. Since these two points do not depend on N, the above description can be more or less generalized to N-electron rings. For example, when the narrow ring contains N electrons, instead of equation (3), the eigenenergy reads

$$E = \frac{1}{N} G(L + N\Phi)^2 + E_{\text{int}} - S_Z \mu \Phi. \tag{22}$$

Instead of equation (6), the total current becomes

$$J = \frac{1}{4\pi} g \int \prod_i \mathrm{d}\theta_i \left[\Psi^* \left(-\mathrm{i} \sum_j^N \frac{\partial}{\partial \theta_j} + N\Phi \right) \Psi + \text{c.c.} \right]. \tag{23}$$

When the arguments are changed to θ_C together with the set of internal degrees of freedom, due to $\sum_j \frac{\partial}{\partial \theta_j} = \frac{\partial}{\partial \theta_C}$ and the separability of Ψ, the above integration can be performed analytically. Thus we have a simple analytical form

$$J = g(L + N\Phi)/2\pi \tag{24}$$

which is a generalization of equation (7). For the ground state, L_o and $N\Phi$ cancel with each other to a great extent. Therefore the current J_o does not increase with N linearly as one might suggest.

Instead of equation (17), we have a more general formula

$$\Delta_{\hbar\omega} = 2hJ_o/N \tag{25}$$

where $\Delta_{\hbar\omega}$ is the energy difference of the two photons absorbed by the ground state during the dipole transition. The final states here are the two possessing the same internal state and have $L_{(f)} = L_o \pm 1$. This formula holds, obviously, also for the reverse process.

Nonetheless, when $N \geqslant 3$, the internal states are complicated and they deserve to be further studied. Furthermore, in practice, most rings are not very narrow. How the results of this paper are affected by the width of the ring (or in general by the 2D confinement potential) deserves to be further studied.

Acknowledgment

This work was supported by the NSFC of China under the grant 10574163.

References

[1] Lorke A, Luyken R J, Govorov A O, Kotthaus J P, Garcia J M and Petroff P M 2000 *Phys. Rev. Lett.* **84** 2223
[2] Keyser U F, Fühner C, Borck S, Haug R J, Bichler M, Abstreiter G and Wegscheider W 2003 *Phys. Rev. Lett.* **90** 196601
[3] Mailly D, Chapelier C and Benoit A 1993 *Phys. Rev. Lett.* **70** 2020
[4] Fuhrer A, Lüscher S, Ihn T, Heinzel T, Ensslin K, Wegscheider W and Bichler M 2001 *Nature* **413** 822
[5] Viefers S, Koskinen P, Singha Deo P and Manninen M 2004 *Physica* E **21** 1
[6] Niemelä K, Pietiläinen P, Hyvönen P and Chakraborty T 1996 *Europhys. Lett.* **36** 533
[7] Korkusinski M, Hawrylak P and Bayer M 2002 *Phys. Status Solidi* b **234** 273
[8] Barticevic Z, Fuster G and Pacheco M 2002 *Phys. Rev.* B **65** 193307
[9] Ferconi M and Vignale G 1994 *Phys. Rev.* B **50** 14722
[10] Serra Li, Barranco M, Emperador A, Pi M and Lipparini E 1999 *Phys. Rev.* B **59** 15290
[11] Emperador A, Pederiva F and Lipparini E 2003 *Phys. Rev.* B **68** 115312
[12] Bao C G, Huang G M and Liu Y M 2005 *Phys. Rev.* B **72** 195310
[13] Hansen A E, Kristensen A, Pedersen S, Sorensen C B and Lindelof P E 2002 *Physica* E **12** 770
[14] Moulopoulos K and Constantinou M 2004 *Phys. Rev.* B **70** 235327
[15] Planelles J, Climente J I and Movilla J L 2005 *Preprint* cond-mat/0506691
[16] Climente J I and Planelles J 2005 *Phys. Rev.* B **72** 155322
[17] Govorov A O, Ulloa S E, Karrai K and Warburton R J 2002 *Phys. Rev.* B **66** 081309
[18] Wendler L, Fomin V M, Chaplik A V and Govorov A O 1996 *Phys. Rev.* B **54** 4794
[19] Bayer M, Korkusinki M, Hawrylak P, Gutbrod T, Michel M and Forchel A 2003 *Phys. Rev. Lett.* **90** 186801
[20] Barticevic Z, Pacheco M and Latge A 2000 *Phys. Rev.* B **62** 6963
[21] Chakraborty T and Pietilainen P 1994 *Phys. Rev.* B **50** 8460
[22] Rose M E 1955 *Multipole Fields* (New York: Wiley)
[23] Poulsen M D and Madsen L B 2005 *Phys. Rev.* A **72** 042501
[24] Koskinen M, Manninen M, Mottelson B and Reimann S M 2001 *Phys. Rev.* B **63** 205323